WARSAW UNIVERSITY OF TECHNOLOGY Index 351733
FACULTY OF CIVIL ENGINEERING
COMMITTEE FOR CIVIL AND WATER ENGINEERING
POLISH ACADEMY OF SCIENCES ISSN 1230-2945

DOI: 10.24425/ace.2024.149865

ARCHIVES OF CIVIL ENGINEERING

Vol. LXX ISSUE 2 2024

pp. 309 –322

Research paper

Static liquefaction as a form of material instability in element test simulations of granular soil

Krzysztof Sternik[1]

Abstract: Static liquefaction is a form of unstable behaviour of granular soil. It is most common in saturated loose sands under monotonically loaded undrained conditions. Predicting static liquefaction using an elastic-plastic model that incorporates the non-associated plastic flow rule and strain hardening is possible. The article briefly describes the unstable behaviour of saturated sand in undrained conditions under a monotonic load. A simple elastic-plastic model with deviatoric hardening and a Drucker–Prager load surface is presented. The constitutive relationships were programmed in a Python script. Simulations of triaxial tests under mixed stress-strain control demonstrated the model's ability to predict various undrained sand responses, including fully stable responses (no liquefaction) and partial and complete liquefaction under triaxial compression and tension. Predicting static liquefaction is possible by properly selecting the proportions of the parameters involved in plastic potential and loading functions and the parameter A used in the deviatoric hardening rule of hyperbolic type.

Keywords: constitutive model, element test, numerical simulation, static liquefaction

[1]PhD., Eng., Silesian University of Technology, Faculty of Civil Engineering, ul. Akademicka 5, 44-100 Gliwice, Poland, e-mail: Krzysztof.Sternik@polsl.pl, ORCID: 0000-0002-8354-6724

1. Introduction

In geomaterials, especially soils, two modes of failure may occur before the limit stress condition is reached: localised and diffuse. The first occurs when a strong concentration of strain increments is generated in the initially smooth distribution of the strain field. This concentration comprises a narrow zone (shear band) while, at the same time, a material beside this zone experiences unloading.

The second one does not exhibit such clear shear surfaces. Material changes gradually from solid-like into fluid-like, comprising a much larger volume than in shear bands. Many points reach a failure state through a chaotic displacement field without any particular geometrical pattern. Both types of failure modes may occur in soil slopes. Many landslides exhibit clear shear planes, but diffuse failure occurs particularly in slopes inclined even at a very low angle (as low as 8°). In that case, soil mass moves downhill as a flow slide or mudflow.

Static liquefaction is an example of a diffuse mode of failure. It occurs mainly in loose sands when the effective mean pressure decreases to zero. Liquefaction of soils may lead to flow slides, i.e., shallow slope failures triggered by saturation of the ground and groundwater seepage. This phenomenon has been extensively studied both experimentally and theoretically. Theoretical works aim at formulating elasto-plastic constitutive equations capable of predicting the behaviour of granular materials in undrained conditions.

In the past decades, the liquefaction of soils has been extensively studied experimentally and theoretically. Experimental works on static liquefaction originate from the works of Castro [1] and Castro and Poulos [2], a review article by Ishihara [3] as well as more recent papers by Yamamuro and Lade [4–6], Świdziński [7], Sawicki and Świdziński [8]. Theoretical works aim at formulating elasto-plastic constitutive equations capable of describing the behaviour of granular materials in undrained conditions. Constitutive models exhibiting this feature are of different origins:

- elasto-plastic models based on Critical State Soil Mechanics assumptions, e.g. [9–13];
- Lade's model with a double plastic potential [14];
- generalized plasticity models [15–18];
- incremental octo-linear model [19];
- incrementally non-linear model [20];
- hypoplastic models, e.g. [21, 22].

Static liquefaction can be predicted within the framework of elastoplasticity if two conditions are met:

1. a model must incorporate hardening and
2. the flow rule must be non-associated.

The article aims to present the capability of the elastic-plastic model with the Drucker–Prager failure criterion and the deviatoric hardening rule to predict static liquefaction. The model assumes a non-associated flow rule with the plastic potential function of the original Cam clay type.

The results of element tests in the axisymmetric condition using the analysed model will be presented, i.e. the results of the calculation of the model's response to an enforced load under mixed control conditions with various constant horizontal total stresses and forced vertical strain in compression or extension.

2. Testing in the triaxial apparatus

One of the significant advantages of the triaxial apparatus is the control provided over drainage from the sample. When no drainage is required (i.e., in undrained tests), solid end caps are used at the top and the bottom of a sample. The end caps are provided with porous plates and drainage channels when drainage is required. It is also possible to monitor pore-water pressures during a test. In drained conditions, a sample can change its volume without pore-water pressure generation, and total stresses σ are equal to effective stresses σ'. In undrained conditions, the volume of a sample remains constant. For a fully saturated sample of granular soil, the relationship between total stresses, effective stresses and pore-water pressure u in vector form follows Terzaghi's principle:

$$\boldsymbol{\sigma} = \boldsymbol{\sigma}' + \mathbf{1}u \tag{2.1}$$

where $\mathbf{1} = [1, 1, 1, 0, 0, 0]^T$.

In the above formula the excess of pore-water pressure as well as compressive stresses are positive.

Test results are usually represented by the invariants of stress and strain, which in axi-symmetric conditions take the form:

- mean stress $p = \frac{1}{3}(\sigma_a + 2\sigma_r)$
- deviatoric stress $q = \sigma_a - \sigma_r$
- volumetric strain $\varepsilon_v = \varepsilon_a + 2\varepsilon_r$
- shear strain $\varepsilon_q = \frac{2}{3}(\varepsilon_a - \varepsilon_r)$

where the subscript a stands for axial (vertical), and r stands for radial (horizontal).

In undrained conditions $\varepsilon_v = 0$, so $\varepsilon_q = \varepsilon_a$.

Conventional triaxial compression can be represented by a straight total stress path with a slope $\eta = q/p = 3$ in the stress invariant space. In undrained conditions increasing pore-water pressure bends an effective stress path towards failure condition (critical stress line).

3. Static liquefaction

The critical state was defined by Roscoe et al. [13] as the state at which soil continues to deform at constant stress and constant void ratio. Jefferies and Been [9, 10] point out that the volume of soil element is constant, and there is no tendency to change the state. Casagrande first introduced the term critical state in 1936 [23] regarding a critical void ratio. Next, Castro [1] conducted triaxial tests on loose samples, which resulted in a well-defined steady state at the end of the tests. Castro termed the relationship between the critical void ratio and the mean stress a steady state line.

Poulos [24] formally defined the steady state line: the steady state of deformation for any mass of particles is that state in which the mass is continuously deforming at constant volume, normal effective stress, and shear stress and velocity.

Despite the discussion about whether the critical state and steady state lines are the same [2, 24–27], Been et al. [25] found that for practical purposes, their equivalence could be assumed.

Undrained shearing is carried out in the triaxial apparatus, usually after isotropic consolidation. The typical behaviour of sand in triaxial undrained compression is given in Fig. 1. Conclusions from this figure also apply to the undrained behaviour during shearing after anisotropic consolidation.

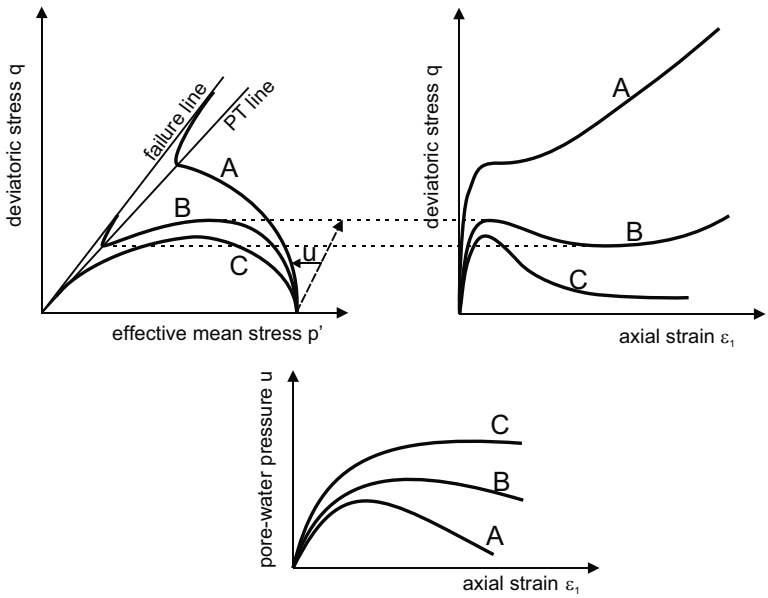

Fig. 1. Reaction of granular soil to undrained loading

During shearing in drained conditions, the volume of the sample varies depending on its initial state. Loose sand decreases its volume, whereas dense sand contracts a little at the onset of shearing and then dilates. Thus, sand can be contractive or dilative. As Świdziński points out in [7], the terms loose and dense are not quite adequate since the behaviour of sand depends not only on the initial void ratio but also on the effective mean pressure. Thus, terms contractive or dilative are more appropriate.

Depending on the initial state of sand, three types of undrained behaviour are observed (Fig. 1). Dense sand (initially in the dilative state – curve A) exhibits constant growth of the deviatoric stress (the strength increases) under monotonic loading. It is accompanied by the initial development of pore-water pressure and the subsequent drop. The local minimum of the deviatoric stress is not observed. Instead, a point of inflexion on the stress path is observed.

Curve B represents the undrained behaviour of initially loose (contractive) sand. In this case, the stress path exhibits a local peak of deviatoric stress accompanied by increased pore-water pressure and a drop in the effective mean stress. Then, after a slight fall of

deviatoric stress, an abrupt turn of the stress path towards increasing strength occurs. The pore-water pressure drops simultaneously (effective mean stress rises). The local minimum of deviatoric stress corresponds to the so-called phase transformation [3, 27, 28]). Under the phase transformation, the transition from contracting to dilating behaviour occurs (PT line in Fig. 1). This behaviour is called limited liquefaction. The state of stress corresponding to the local minimum of deviatoric stress is called the quasi-steady state [23].

Curve C in Fig. 1 represents static liquefaction [1, 7, 29–31]. It occurs in basically undrained shearing of contractive (initially loose) sands. During monotonic loading, pore-water pressure increases and the effective mean stress drops. The stress path passes the peak deviatoric value (peak strength) and then decreases. Both deviatoric and effective mean stress eventually reach residual values while constantly increasing deformation.

4. Description of the model

The model applied in the simulations assumes deviatoric hardening, which means that the loading surface is of the type

$$f\left(p, q, \varepsilon_q^p\right) = 0 \tag{4.1}$$

where ε_q^p is the accumulated plastic shear strain, p is the function of the first invariant of the stress tensor, and q is the function of the second invariant of the stress deviator (the definitions of both in axisymmetry are given above).

The formulation assumes non-associated flow rule, i.e.

$$\mathrm{d}\boldsymbol{\varepsilon} = \mathrm{d}\lambda \frac{\partial g}{\partial \boldsymbol{\sigma}} \wedge g = g\left(\boldsymbol{\sigma}\right) = \text{const} \tag{4.2}$$

where $d\lambda$ is the plastic multiplier and g is the plastic potential function.

The loading surface for granular soils is given by the equation (Fig. 2)

$$f = q - \eta p' = 0 \tag{4.3}$$

and the deviatoric hardening is of the hyperbolic type

$$\eta(\varepsilon_q^p) = \eta_0 + \left(\eta_f - \eta_0\right) \frac{\varepsilon_q^p}{\varepsilon_q^p + A} \tag{4.4}$$

where η_0 is the initial stress ratio, η_f is the ultimate stress ratio at failure, A is the material constant.

In the stress space, the Drucker–Prager cone represents the loading surface, whose element's slope varies from $\eta_0 = q_0/p_0'$ to $\eta_f = q_f/p_f'$. The initial slope q_0/p_0' represents the starting point of the analysis. To avoid singularities during calculations, compression/extension simulations after isotropic consolidation in the triaxial apparatus when

$q_0 = 0$, η_0 should be a small number. In the case of anisotropic consolidation corresponding to in situ conditions, η_0 takes on the value

$$\eta_0 = \frac{3(1 - K_0)}{1 + 2K_0} \tag{4.5}$$

where K_0 is the coefficient of earth pressure at rest.

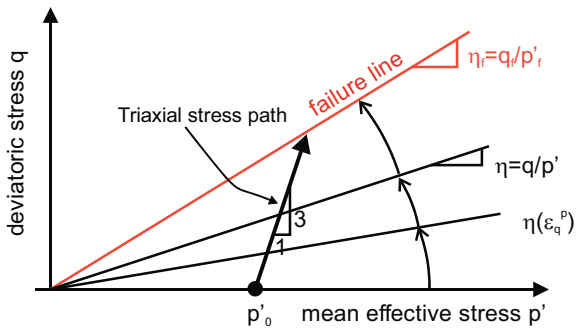

Fig. 2. Evolution of the loading surface with plastic straining

The plastic potential function is chosen in such a way as to ensure a continuous transition from contractive to dilative behaviour during the deformation process. This can be achieved by defining plastic potential in a form similar to that used in Cam clay's original formulation, i.e.

$$g = q + \eta_c p' \ln \frac{p'}{\overline{p}} = 0 \tag{4.6}$$

where η_c is a material constant which represents zero-dilatancy line.

In the above equation, $\overline{p}$ is defined by the condition $g\,(p', q) = 0$ for the current stress state on the loading surface. Note that the partial derivative responsible for plastic volumetric changes

$$\frac{\partial g}{\partial p'} = \eta_c \left(\ln \frac{p'}{\overline{p}} + 1 \right) = \eta_c - \eta \tag{4.7}$$

so that $\eta = \eta_c$ when $\partial g / \partial p' = 0$ and $\mathrm{d}\varepsilon_v^p = 0$. If $\eta < \eta_c$ there is $\mathrm{d}\varepsilon_v^p > 0$, which means contraction, while if $\eta > \eta_c$ there is $\mathrm{d}\varepsilon_v^p < 0$, which means dilatancy.

Figure 3 schematically shows the deviatoric hardening model and plastic potential in triaxial compression in $p - q$ space.

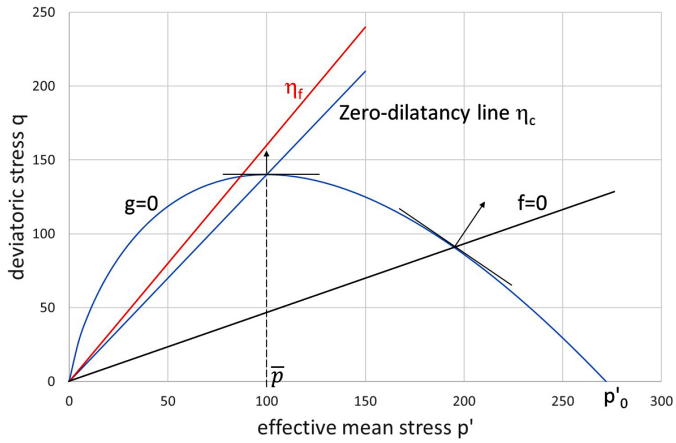

Fig. 3. Plastic potential function, loading function incremental plastic strain directions

Inside the yield locus the non-linear elastic behaviour is assumed with the well-known elastic matrix

$$\mathbf{D}^e = \frac{E_{\text{sec}}}{(1+\nu)(1-2\nu)} \begin{bmatrix} 1-\nu & \nu & \nu & 0 & 0 & 0 \\ \nu & 1-\nu & \nu & 0 & 0 & 0 \\ \nu & \nu & 1-\nu & 0 & 0 & 0 \\ 0 & 0 & 0 & \dfrac{1-2\nu}{2} & 0 & 0 \\ 0 & 0 & 0 & 0 & \dfrac{1-2\nu}{2} & 0 \\ 0 & 0 & 0 & 0 & 0 & \dfrac{1-2\nu}{2} \end{bmatrix} \tag{4.8}$$

where ν is Poisson ratio and E_{sec} is the stress dependent secant elastic modulus.

At the beginning of the analysis, when volumetric strain $\Delta\varepsilon_v^e = 0$

$$E = E_{\text{ref}} \left(\frac{\max(p', p_L)}{\sigma_{\text{ref}}} \right)^m \tag{4.9}$$

where p_L is the limit mean stress, m is a material constant, and σ_{ref} is the reference stress usually taken as the atmospheric pressure.

At a more advanced stage of analysis, when $\Delta\varepsilon_v^e \neq 0$

$$E_{\text{sec}} = \beta_K \frac{p'_{n+1} - p'_n}{\Delta\varepsilon^e_{v,n+1}} \tag{4.10}$$

$$\beta_K = \frac{1}{3(1-2\nu)} \tag{4.11}$$

where p'_{n+1} and p'_n are the searched (trial) and converged (starting value of p' before the applied load increment) mean stresses respectively. $\Delta\varepsilon^e_{v,n+1}$ is the trial elastic increment of the volumetric strain.

For the non-associated flow rule, the constitutive relation in drained conditions are given in the usual manner [32]:

$$\mathrm{d}\boldsymbol{\sigma}' = \mathbf{D}^{ep}\mathrm{d}\boldsymbol{\varepsilon} \tag{4.12}$$

$$\mathbf{D}^{ep} = \mathbf{D}^{e} - \frac{1}{H}\left(\mathbf{D}^{e}\left(\frac{\partial g}{\partial \boldsymbol{\sigma}}\right)\left(\frac{\partial f}{\partial \boldsymbol{\sigma}}\right)^{T}\mathbf{D}^{e}\right) \tag{4.13}$$

$$H = H_e + H_p; \quad H_e = \left(\frac{\partial f}{\partial \boldsymbol{\sigma}}\right)^{T}\mathbf{D}^{e}\left(\frac{\partial g}{\partial \boldsymbol{\sigma}}\right); \quad H_p = -\frac{\partial f}{\partial \varepsilon_q^p}\frac{\partial g}{\partial q} \tag{4.14}$$

The constitutive equation must be complimented for fully saturated soil in undrained conditions based on Terzaghi's rule. The pore water pressure increase due to loading is

$$\mathrm{d}u = \frac{K^f}{n}\mathrm{d}\varepsilon_v = \xi\mathrm{d}\varepsilon_v \tag{4.15}$$

where K^f is the bulk modulus of water and n is porosity.

Thus

$$\mathrm{d}\boldsymbol{\sigma} = \mathbf{D}^{ep}\mathrm{d}\varepsilon + \mathbf{1}\mathrm{d}u = \left(\mathbf{D}^{ep} + \xi\mathbf{1}\mathbf{1}^{T}\right)\mathrm{d}u \tag{4.16}$$

Therefore, the model requires the declaration of six parameters: E_{ref}, ν, m, η_f, η_c, A and additionally σ_{ref} and p_L.

5. Simulations of triaxial compression and extension

5.1. Assumptions

To present the capability of the model to predict static liquefaction of soil in undrained conditions, the assumptions given below were made.

Three total confining pressures were considered $\sigma_r = 100, 300, 500$ kPa, which were kept constant throughout the simulations.

The following elastic properties were assumed: $E_{\mathrm{ref}} = 80000$ kPa, $m = 0.5$, $\nu = 0.2$, $\sigma_{\mathrm{ref}} = 100$ kPa. The elastic modulus was kept constant for the mean stress $p' < p_L = 10$ kPa.

The ultimate stress ratio at failure $\eta_f = 1.6$.

The simulation program was carried out using a script in Python by Prof Andrzej Truty from the Cracow University of Technology, assuming that the mechanical reaction to triaxial compression and extension in undrained conditions would be tested. The element tests were carried out under mixed control conditions: the total horizontal stress was kept constant, and the vertical strain increments were set to a maximum value of 10%. Thus, the answer of the constitutive model to the applied load was vertical stresses and horizontal strains.

In the performed calculations, the influence of the difference between η_c and η_f on changes in effective stresses and shear curves was checked. The effect of parameter A in the deviatoric hardening law on the mechanical reaction of the constitutive model was also studied.

To study the model's reaction, three values of zero dilatancy line gradient: $\eta_c = 1.4, 1.5, 1.65$ were assumed, of which two are lower than $\eta_f = 1.6$. In those simulations, $A = 0.0035$ was assumed. Also, three values of the parameter $A = 0.0015, 0.0035, 0.0055$ accompanied by $\eta_c = 1.5$ were taken in other simulations.

5.2. Results

The results of simulations of triaxial compression and extension for the set of parameters representing dense / medium dense sand are presented in Fig. 4 and 5. Since η_c is much smaller than η_f, these results generally do not exhibit liquefaction. Only in the case of the simulation carried out for the horizontal stress $\sigma_r = 100$ kPa, an unstable state is revealed, represented by a fragment of the effective stress path, which starts from the point of peak deviatoric stress to the phase transformation point, where the stress path changes direction and starts moving away from the origin of the coordinate system. This phase is also evident in the shear curve for $\sigma_r = 100$ kPa, where the deviatoric stress decreases slightly before increasing again (Fig. 5). The same mechanical reaction occurs in both compression and extension.

In Fig. 6 and 7, the results are compared for all the assumed values of η_c. There can be seen that no liquefaction occurs when $\eta_f > \eta_c$, while complete liquefaction can be predicted for $\eta_f \leqslant \eta_c$. Partial liquefaction occurs when η_c is close enough to η_f. In the case of complete liquefaction, the paths of effective stresses tend towards the beginning of the $p - q$ system (Fig. 6), and the shear curves descend (Fig. 7) for all horizontal stresses σ_r.

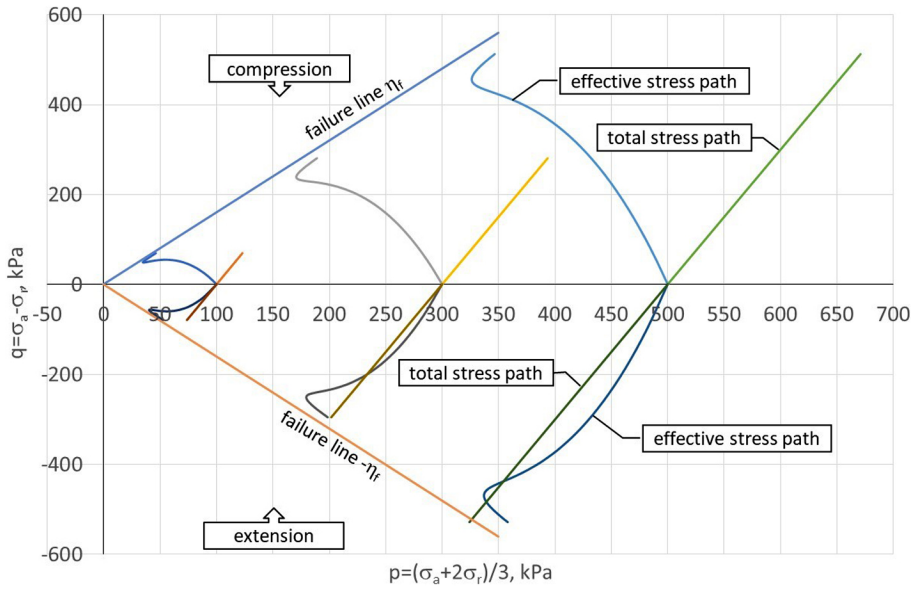

Fig. 4. Total and effective stress paths for triaxial compression and extension for $\eta_c = 1.4$

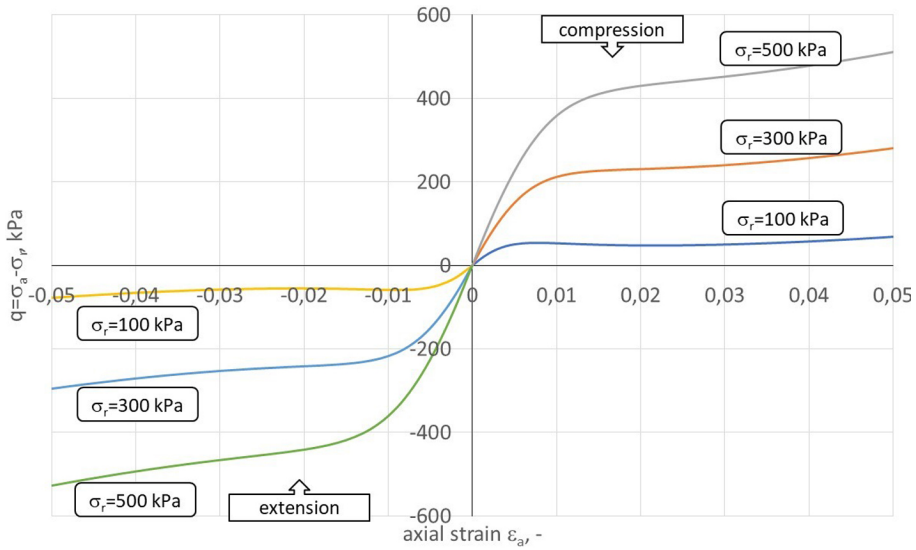

Fig. 5. Shear curves for $\eta_c = 1.4$

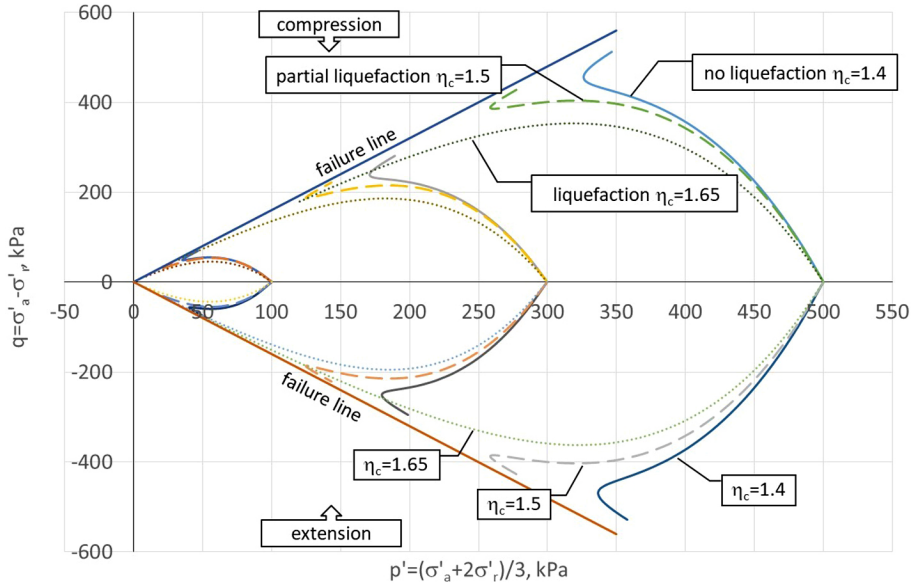

Fig. 6. Stress paths for assumed values of η_c and horizontal stresses σ_r

Similar types of response to the undrained load, as for the changing ratio η_c/η_f, are obtained for different values of parameter A. For the smallest value of A, one does not observe liquefaction even for $\sigma_r = 100$ kPa. Increasing A leads to an increasingly pronounced phase of unstable behaviour, eventually leading to liquefaction.

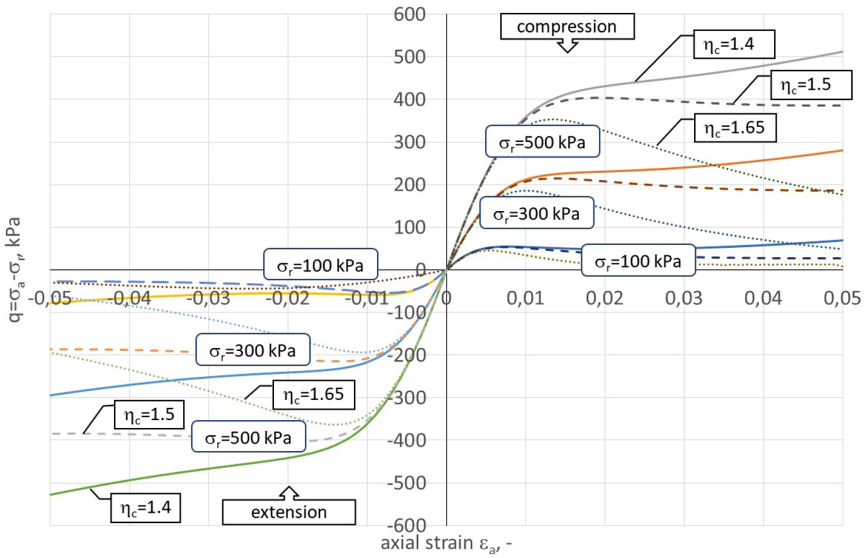

Fig. 7. Comparison of shear curves for assumed values η_c and horizontal stresses σ_r

It should be noted that increasing A leads to flatter effective stress paths (Fig. 8) and a more significant reduction of the initial stiffness (Fig. 9) for all σ_r. Changes in η_c do not cause the stress paths to diverge so quickly at the same σ_r (Fig. 6), and the initial stiffnesses are almost identical (Fig. 7) in compression and extension.

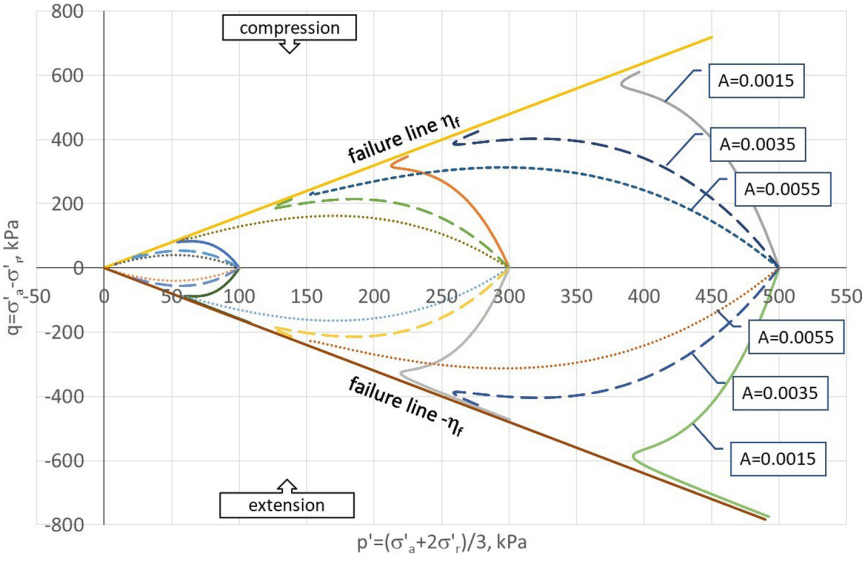

Fig. 8. Stress paths for different values of the parameter A

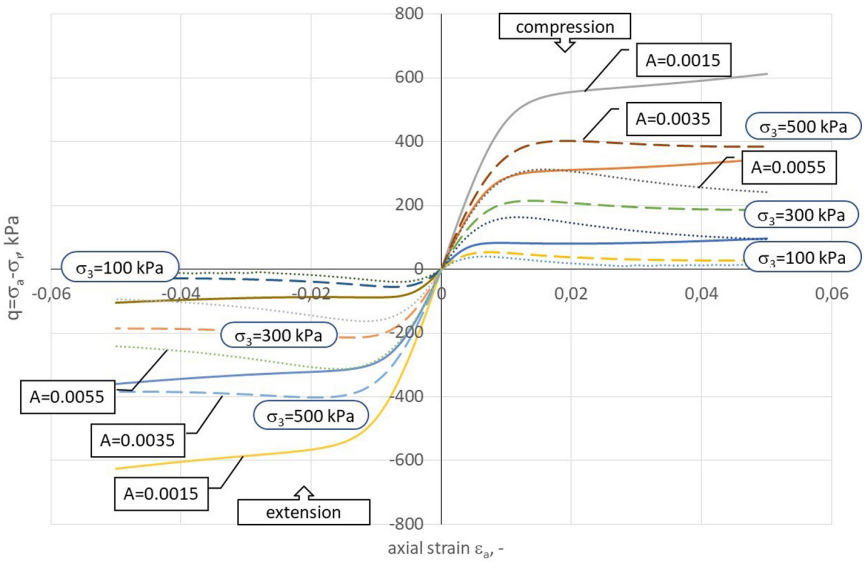

Fig. 9. Shear curves for different values of the parameter A

6. Discussion of the results and conclusions

The response of the presented model shows that static liquefaction can be achieved in two ways:

– suitably choosing the difference between η_c and η_f,

– suitably selecting the value of parameter A.

In the case of partial liquefaction, the prevailing mechanism in volume changes is plastic densification, so a progressive increase in pore-water pressure is observed before failure. The failure mechanism is associated with excessive deformations at a constant level of vertical stresses.

In the case where $\eta_c \geq \eta_f$, the plastic contraction is predicted in the entire load range before reaching the failure envelope. Under undrained conditions, this means a continuous increase in pore pressure and migration of the effective stress path towards the origin of the $p'q$ stress space. After passing the point of the maximum q, the soil characteristics become unstable, leading to complete liquefaction.

The presented model has some limitations. One of them is that, except for the case $\eta_c = \eta_f$, the effective stress path asymptotically approaches the Drucker–Prager failure envelope but does not reach it. Thus, the critical state cannot be reached. Volume changes do not disappear, and either volumetric expansion ($\eta_c < \eta_f$) or volumetric compression ($\eta_c > \eta_f$) occurs indefinitely. Nor can the model predict the post-peak softening observed when dense sands are sheared in drained conditions. These deficiencies can be removed by introducing a variable η_f depending on the current state of stress and soil density as done by Muir Wood [33].

References

[1] G. Castro, "Liquefaction and cyclic mobility of saturated sands", *Journal of the Geotechnical Engineering Division*, vol. 101, no. 6, pp. 551–569, 1975, doi: 10.1061/AJGEB6.0000173.

[2] G. Castro and S.J. Poulos, "Factors affecting liquefaction and cyclic mobility", *Journal of the Geotechnical Engineering Division*, vol. 103, no. 6, pp. 501–516, 1977, doi: 10.1061/AJGEB6.0000433.

[3] K. Ishihara, "Liquefaction and flow failure during earthquakes", *Géotechnique*, vol. 43, no. 3, pp. 351–415, 1993, doi: 10.1680/geot.1993.43.3.351.

[4] J.A. Yamamuro and P.V. Lade, "Static liquefaction of very loose sands", *Canadian Geotechnical Journal*, vol. 34, no. 6, pp. 905–917, 1997, doi: 10.1139/t97-057.

[5] J.A. Yamamuro and P.V. Lade, "Steady state concepts and static liquefaction of silty sands", *Journal of Geotechnical and Geoenvironmental Engineering*, vol. 124, no. 9, pp. 868–877, 1998, doi: 10.1061/(ASCE)1090-0241(1998)124:9(868).

[6] J.A. Yamamuro and P.V. Lade, "Experiments and modelling of silty sands susceptible to static liquefaction", *Mechanics of Cohesive-Frictional Materials*, vol. 4, no. 6, pp. 545–564, 1999, doi: 10.1002/(SICI)1099-1484(199911)4:6<545::AID-CFM73>3.0.CO;2-O.

[7] W. Świdziński, *Compaction and liquefaction mechanisms of non-cohesive soils*. Gdańsk: Wydawnictwo IBW PAN, 2006 (in Polish).

[8] A. Sawicki and W. Świdziński, "Modelling the pre-failure instabilities of sand", *Computers and Geotechnics*, vol. 37, no. 6, pp. 781–788, 2010, doi: 10.1016/j.compgeo.2010.06.004.

[9] M.G. Jefferies, "Nor-Sand: a simple critical state model for sand", *Géotechnique*, vol. 43, no. 1, pp. 91–103, 1993, doi: 10.1680/geot.1993.43.1.91.

[10] M.G. Jefferies and K. Been, *Soil Liquefaction. A critical state approach*. London and New York: Taylor & Francis, 2015, doi: 10.1201/b19114.

[11] X.S. Li, Y.F. Dafalias, and Z.-L.Wang, "State dependent dilatancy in critical state constitutive modelling of sand", *Canadian Geotechnical Journal*, vol. 36, no. 4, pp. 599–611, 1999, doi: 10.1139/t99-029.

[12] R. Nova and D.M. Wood, "A constitutive model for sand in triaxial compression", *International Journal of Numerical and Analytical Methods in Geomechanics*, vol. 3, no. 3, pp. 255–278, 1979, doi: 10.1002/nag.1610030305.

[13] K. Roscoe, A.N. Schofield, and C.P. Wroth, "On the yielding of soils", *Géotechnique*, vol. 8, no. 1, pp. 22–53, 1958, doi: 10.1680/geot.1958.8.1.22.

[14] P.V. Lade, "Elastoplastic stress-strain theory for cohesionless soil with curved yield surfaces", *International Journal of Solids and Structures*, vol. 13, no. 11, pp. 1019–1035, 1977, doi: 10.1016/0020-7683(77)90073-7.

[15] M. Pastor, O.C. Zienkiewicz, and A.H.C. Chan, "Generalized plasticity and the modelling of soil behaviour", *International Journal of Numerical and Analytical Methods in Geomechanics*, vol. 14, no. 3, pp. 151–190, 1990, doi: 10.1002/nag.1610140302.

[16] M. Pastor, O.C. Zienkiewicz, and K.H. Leung, "A simple model for transient soil loading in earthquake analysis. II: Non-associative model for sands", *International Journal of Numerical and Analytical Methods in Geomechanics*, vol. 9, no. 5, pp. 477–498, 1985, doi: 10.1002/nag.1610090506.

[17] O.C. Zienkiewicz and Z. Mróz, "Generalized plasticity formulation and application to geomechanics", in *Mechanics of Engineering Materials*, C. S. Desai and R. H. Gallagher, Eds. New York: John Wiley and Sons, 1984.

[18] O.C. Zienkiewicz, K.H. Leung, and M. Pastor, "A simple model for transient soil loading in earthquake analysis. I: Basic model and its application", *International Journal of Numerical and Analytical Methods in Geomechanics*, vol. 9, no. 5, pp. 953–976, 1985, doi: 10.1002/nag.1610090505.

[19] F. Darve and S. Labanieh, "Incremental constitutive law for sands and clays: simulation of monotonic and cyclic tests", *International Journal of Numerical and Analytical Methods in Geomechanics*, vol. 6, no. 2, pp. 243–275, 1982, doi: 10.1002/nag.1610060209.

[20] F. Darve, "Incrementally non-linear constitutive relationships", in *Geomaterials constitutive equations and modelling*, F. Darve, Ed. London: Elsevier Applied Science, 1990, pp. 213–238, doi: 10.1201/9781482296532.

[21] D. Kolymbas, "An outline of hypoplasticity", *Archive of Applied Mechanics*, vol. 61, pp. 143–151, 1991, doi: 10.1007/BF00788048.

[22] W. Wu and A. Niemunis, "Failure criterion, flow rule and dissipation function derived from hypoplasticity", *Mechanics of Cohesive-Frictional Materials*, vol. 1, no. 2, pp. 145–163, 1996, doi: 10.1002/(SICI)1099-1484(199604)1:2<145::AID-CFM8>3.0.CO;2-9.

[23] A. Casagrande, "Characteristics of cohesionless soils affecting the stability of earth fills", *Journal of Boston Society of Civil Engineers*, vol. 23, pp. 257–276, 1936.

[24] S.J. Poulos, "The steady state of deformation", *Journal of Geotechnical Engineering Division*, vol. 107, no. 5, pp. 553–562, 1981, doi: 10.1061/AJGEB6.0001129.

[25] K. Been, M.G. Jefferies, and J. Hachey, "The critical states of sands", *Géotechnique*, vol. 41, no. 3, pp. 365–381, 1991, doi: 10.1680/geot.1991.41.3.365.

[26] J. A. Sladen, R.D. D'Hollander, and J. Krahn, "The liquefaction of sands, a collapse surface approach", *Canadian Geotechnical Journal*, vol. 22, no. 4, pp. 564–578, 1985, doi: 10.1139/t85-076.

[27] Y.P. Vaid, E.K.F. Chung, and R.H. Kuerbis, "Stress path and steady state", *Canadian Geotechnical Journal*, vol. 27, no. 1, pp. 1–7, 1990, doi: 10.1139/t90-001.

[28] R. Verdugo and K. Ishihara, "The steady state of sandy soils", *Soils and Foundations*, vol. 36, no. 2, pp. 81–91, 1996, doi: 10.3208/sandf.36.2_81.

[29] A. Casagrande, "Liquefaction and cyclic deformation of sands, a critical review", in *Proceedings of the* 5^{th} *Pan-American Conference on Soil Mechanics and Foundation Engineering*, Harvard Soil Mechanics Series, no. 88. Cambridge: Harvard University, 1979, pp. 79–133.

[30] M.B. de Groot, M.D. Bolton, P. Foray, P. Meijers, A.C. Palmer, R. Sandven, A. Sawicki, and T.C. Teh, "Physics of liquefaction phenomena around marine structures", *Journal of Waterway, Port, Coastal, and Ocean Engineering*, vol. 132, no. 4, pp. 227–243, 2006, doi: 10.1061/(ASCE)0733-950X(2006)132:4(227).

[31] K. Ishihara, F. Tatsuoka, and V. Yasuda, "Undrained deformation and liquefaction of sand under cyclic stresses", *Soils and Foundations*, vol. 15, no. 1, pp. 29–44, 1975, doi: 10.3208/sandf1972.15.29.

[32] D.C. Drucker, R.E. Gibson, and D.J. Henkel, "Soil mechanics and work-hardening theories of plasticity", *Transactions of ASCE*, vol. 122, no. 1, pp. 338–346, 1957, doi: 10.1061/TACEAT.0007430.

[33] D. Muir Wood, *Geotechnical modelling*. London and New York: Spon Press Taylor & Francis Group, 2004, doi: 10.1201/9781315273556.

Statyczne upłynnienie jako forma niestabilności materiału w symulacjach testów elementowych gruntu niespoistego

Słowa kluczowe: model konstytutywny, symulacja numeryczna, test elementowy, upłynnienie statyczne

Streszczenie:

Statyczne upłynnienie jest formą niestabilnego zachowania się gruntu niespoistego. Najczęściej występuje w nasyconych piaskach luźnych w warunkach bez odpływu wody obciążonych monotonicznie. Możliwe jest prognozowanie statycznego upłynnienia przy użyciu sprężysto-plastycznego modelu, w którym uwzględnia się niestowarzyszone prawo płynięcia plastycznego i wzmocnienie odkształceniowe. W pracy przedstawiono krótki opis niestabilnego zachowania się piasku nasyconego w warunkach bez odpływu pod obciążeniem monotonicznym. Zaprezentowano prosty model sprężysto-plastyczny ze wzmocnieniem dewiatorowym i powierzchnią obciążenia Druckera–Pragera. Związki konstytutywne zaprogramowane zostały w skrypcie Python. Symulacje testów trójosiowego ściskania i rozciągania i mieszanej kontroli naprężeniowo-odkształceniowej pokazały zdolność modelu do prognozy różnych reakcji piasku w warunkach bez odpływu, w tym braku upłynnienia, częściowego i pełnego upłynnienia.

Received: 2023-08-03, Revised: 2023-09-22